Desalination and Water Treatment
www.deswater.com

doi: 10.1080/19443994.2015.1027277

57 (2016) 2455–2465
February

Taylor & Francis
Taylor & Francis Group

Adsorption of molecular size fractions of humic acid onto anion-doped TiO_2 specimens

P. Akan[a], N.C. Birben[b,*], M. Bekbolet[b]

[a]*Department of Environmental Engineering, Hacettepe University, 06800 Cankaya, Ankara, Turkey, Tel. +90 312 297 7800; email: apakan@hacettepe.edu.tr*

[b]*Institute of Environmental Sciences, Bogazici University, 34342 Bebek, Istanbul, Turkey, Tel. +90 212 359 7145; Fax: +90 212 359 6946; email: cemrebirben@live.com (N.C. Birben), Tel. +90 212 359 7012; Fax: +90 212 359 6946; email: bekbolet@boun.edu.tr (M. Bekbolet)*

Received 24 October 2014; Accepted 3 March 2015

ABSTRACT

Humic acids (HA) constitute the major fraction of natural organic matter that should be removed during water treatment. Besides conventional treatment methods, application of advanced oxidation processes more specifically photocatalysis has gained much attention in recent decades. Titanium dioxide (TiO_2) is universally recognized as a standard photocatalyst. Since photocatalysis occurs through a surface-oriented mechanism, adsorptive properties of TiO_2 specimens deserve special attention. Moreover, nowadays visible light activated TiO_2 developed by modifications through the use of various dopants has been the subject of numerous investigations. Understanding of the surface interactions prevailing between the anion-doped oxide surface and humic subfractions is important for the determination of the role of humic substances during photocatalysis. The aim of this study was to investigate surface interactions between different molecular size fractions of HA and TiO_2, namely bare TiO_2 and anion-doped TiO_2 (C-doped, N-doped, S-doped and N–S co-doped) specimens. Therefore, adsorption properties of HA and its molecular size fractions onto bare TiO_2 and anion-doped TiO_2 specimens were evaluated by dissolved organic carbon, UV–vis spectral properties, and respective specific UV–vis parameters (SCoA, $SUVA_{365}$, $SUVA_{280}$, and $SUVA_{254}$). Furthermore, the data achieved by adsorption experiments were assessed by Freundlich, Langmuir as well as Dubinin–Radushkevich isotherm models. The results based on varying molecular size fractions of HA displayed remarkable differences with respect to the type of the dopant in comparison to the bare TiO_2 specimen. Consequently, when different molecular size fractions of HA were compared, Freundlich model displayed lower K_F and higher $1/n$ values as well as Langmuir model exhibited maximum quality adsorbable in the presence of lower molecular size fraction. The reason could be also attributed to the compositional properties of HA subfraction along with the alterations in TiO_2 specimens due to doping. From a general perspective, E values in Dubinin–Radushkevich model indicated that the main mechanism for the adsorption of diverse molecular size of HA onto

*Corresponding author.

Presented at the 2nd International Conference on Recycling and Reuse (R&R2014), 4–6 June 2014, Istanbul, Turkey

bare and anion-doped TiO_2 specimens could be mainly attributes to physical forces. Referring to the fundamental aim of the study indicating that the studied dose range of TiO_2 (0.1–1.0 mg mL^{-1}) was selected with respect to the photocatalytically active concentration range, the attained results should be carefully interpreted.

Keywords: Humic acids; Photocatalysis; Natural organic matter; Water treatment

1. Introduction

Natural organic matter (NOM) forming during degradation of plant and animal tissues exists in all surface, ground waters along with soil [1,2]. The most spread NOM existed in the water supplies is humic substances (HS), which are anionic hydrophobic macromolecules possessing surface functional groups containing carboxylic and phenolic groups [3]. HS can be divided into three components: humic acid (HA), fulvic acid (FA), and humin according to their solubility features. HA and FA represent alkali-soluble humus fragments and humin represents the insoluble residue. Humic components are also composed of various fractions displaying different molecular size and weights (e.g. 100 kDa, 30 kDa, and even 500 Da). Presence of HA results in some important problems such as developing color in the water source and forming disinfection by products during chlorination process in the treatment systems. Because of these issues, the removal of HA from water sources has a very high importance [4].

Titanium dioxide (TiO_2), which is used as a standard photocatalyst, is preferred to cope with a great deal of environmental problems such as air purification and wastewater treatment owing to its advantageous features such as photochemical reactivity, high chemical stability, high UV absorption, commercial availability, and inexpensiveness. The band gap energy of TiO_2 points out the wavelength of UV light $\lambda < 400$ nm excluding the beneficial use of visible light region of the electromagnetic spectrum. This situation decreases the ability of TiO_2 as to the decomposition of toxic substances under natural illumination [5]. Some solutions have been found to increase the absorption wavelength range of TiO_2 to the visible region (400 nm $< \lambda <$ 700 nm) without the decrease in photocatalytic activity of TiO_2. One of them is that red shift of the absorption edge of TiO_2 to wavelengths longer than 400 nm can be succeeded by doping TiO_2 with transition metal cations such as chromium, vanadium, iron, and nickel into Ti sites in order to increase photocatalysis efficiency [6]. Another solution is to decrease the band gap energy of TiO_2 by doping with non-metallic elements such as boron, carbon, nitrogen, and sulfur either as mono- or co-doped states [7]. A well-known example of mixed phase TiO_2 is the commercial P-25 material, which consists of approximately 80% anatase and 20% rutile phases. This material has higher chemical stability and photocatalytic activity for oxidative degradation than its pure phase counterparts [8].

Although vast number of research had been dedicated to the use of visible light active photocatalysts, not much attention has been given to the adsorptive properties of these materials towards the substrates under investigation. Due to the surface oriented nature of photocatalysis, adsorption of the substrate onto TiO_2 displays a crucial role in degradation process. Furthermore, excessive adsorption of the substrate onto the photocatalyst is not desired since the extent of the unoccupied surface exposed to light absorption should be enough to produce sufficient amount of reactive oxygen species mainly hydroxyl radicals. With respect to the previously reported studies performed on the photocatalytic degradation of HA using both bare and doped TiO_2 specimens, it was shown that HA could be successfully oxidized to lower molecular weight fractions [9,10]. Therefore, adsorption of HA onto bare TiO_2 and doped TiO_2 specimens requires to be investigated provided that the adsorbent dose should resemble the photocatalytically active range of TiO_2. In that respect, the main aim of this study was directed to the evaluation of the surface interactions existing between the anion-doped oxide surface and HA subfractions.

2. Materials and methods

2.1. Materials

Commercial HA was supplied from Aldrich (Aldrich Company, USA). Stock HA solution (1,000 mg L^{-1}) was prepared using ultrapure water (Millipore Milli-Q plus system, with a resistivity of 18.2 MΩ cm at 25°C). While HA concentration was chosen as 20 mg L^{-1} for 0.45 μm filtered fraction (5.98 mg L^{-1} DOC), HA solution with an initial concentration of 50 mg L^{-1} was employed for preparation of both 100 kDa molecular size fraction and 30 kDa molecular size fractions to achieve enough dissolved organic carbon (DOC) in solution matrix prior to

adsorption onto adsorbents. HA solutions were fractionated using a 50 mL Amicon Model 8010 ultrafiltration stirred cells into two different molecular size fractions (100 and 30 kDa) in order to obtain diverse organic matter contents [11]. HA molecular size fractions were designated as (i) 0.45 μm filtered fraction, (ii) 100 kDa fraction for HA passing through 100 kDa molecular size filter, and (iii) 30 kDa fraction for HA passing through 30 kDa molecular size filter.

TiO_2 P-25 was provided from Evonik Corp. (Germany) (crystal structure: 80% anatase and 20% rutile, nonporous, BET surface area (SA): 55 ± 15 $m^2 g^{-1}$, average particle size: 30 nm, density: 3.8 g mL^{-1}). Anion-doped TiO_2 specimens (i) C-doped, (ii) N-doped, (iii) S-doped, and (iv) N–S co-doped TiO_2 specimens were employed in batch adsorption experiments. Anion-doped specimens were prepared according to a wet impregnation method by Cinar and co-workers in the research laboratories of Department of Chemistry, Yıldız Technical University. Detailed information on the preparation, characterization, and activity testing on these doped TiO_2 specimens have been presented elsewhere by Cinar and colleagues [7,12]. pH_{zpc} of anion-doped TiO_2 specimens was determined by examining the change in zeta potential values with respect to different pH conditions using a Nano/Zetasizer (ZS90, Malvern Instruments Ltd.). Prior to experiments, anion-doped TiO_2 specimens were suspended in a 1 mM NaCl solution followed by pH adjustment either by adding NaOH solution (0.1–1.0 M) or HCl solution (0.1–1.0 M). In addition, all samples were subjected to ultrasonication for 15 min prior to measurements. The nitrogen adsorption/desorption isotherm was obtained at liquid nitrogen temperature 77 K using Quantachrome Nova 2200 e automated gas adsorption system. The specific surface areas were determined using multi-point BET analysis. Properties of bare and doped TiO_2 specimens were presented in Table 1.

2.2. Methodology

Batch adsorption experiments were implemented using 100 mL Erlenmeyer Flasks. Each flask was filled with 25 mL HA solution. Increased amounts of TiO_2 were added to each Erlenmeyer flask starting from 0.1 to 1.0 mg mL^{-1}. Each sample was sonicated before being placed to the shaker for achieving homogeneous distribution of TiO_2 in the slurry. The samples were immersed in a water bath at 25°C which is equipped with a thermostate and a shaking device. Although equilibration time of 6 h was attained for all of the TiO_2 specimens, for practical reasons the flasks were kept shaking for 24 h. Then samples were filtered by 0.45 μm Millipore filter and clear solutions were subjected to analysis. All experiments conducted under neutral pH conditions (pH 6.7–7.0), as is no pH adjustment, were made throughout the experiments since no significant pH change was observed.

UV–vis absorption spectra of HA solutions were recorded using a Perkin Elmer Lambda 35 UV–vis double beam spectrophotometer with Hellma quartz cuvettes of 1.0 cm optical path length. Non-purgeable organic carbon (NPOC) measurements of HA solutions were implemented with a Shimadzu TOC Vwp Total Organic Carbon Analyzer. NPOC was expressed simply as DOC, mg OrgC L^{-1}.

UV–vis absorbance values of different molecular size fractions of HA were determined according to the particular wavelengths that were 436, 365, 280, and 254 nm. Specified UV–vis parameters were represented by (i) $Color_{436}$ representing color-forming moieties at $\lambda = 436$ nm, (ii) UV_{365} representing organic matter content at $\lambda = 365$ nm, (iii) UV_{280} representing aromaticity of the organic matter content at $\lambda = 280$ nm, and (iv) UV_{254} representing organic matter content at $\lambda = 254$ nm. Specific UV–vis parameters were SCoA ($Color_{436}$/DOC), $SUVA_{365}$, (UV_{365}/DOC), $SUVA_{280}$, (UV_{280}/DOC) and, $SUVA_{254}$ (UV_{254}/DOC) [13,14]. Specified and specific parameters of 0.45 μm filtered fraction, 100 kDa fraction and 30 kDa fraction of HA were displayed in Table 2.

3. Results and discussion

Surface interactions between diverse molecular size fractions of HA (0.45 μm filtered fraction, 100 kDa

Table 1
Properties of bare and doped TiO_2 specimens

TiO_2 specimens	pH_{zpc}	Crystallite size (nm)	BET ($m^2 g^{-1}$)
Bare	6.25	22.3	57.55
C-doped	6.01	20.8	56.47
N-doped	5.15	18.8	55.35
S-doped	5.38	18.5	50.16
N–S co-doped	5.61	16.9	45.74

Table 2
Specified and specific UV–vis parameters of HA

Humic acid Parameters	Molecular size fractions		
	0.45 μm filtered	100 kDa	30 kDa
$Color_{436}$ (m^{-1})	9.11	6.61	3.53
UV_{365} (m^{-1})	18.4	14.9	7.97
UV_{280} (m^{-1})	42.2	38.0	21.1
UV_{254} (m^{-1})	48.9	44.9	25.0
DOC (mgL^{-1})	5.981	4.926	2.739
$SCoA_{436}$ (m^{-1} mg^{-1} L)	1.52	1.34	1.29
$SUVA_{365}$ (m^{-1} mg^{-1} L)	3.06	3.02	2.91
$SUVA_{280}$ (m^{-1} mg^{-1} L)	7.05	7.72	7.70
$SUVA_{254}$ (m^{-1} mg^{-1} L)	8.18	9.11	9.13

fraction and 30 kDa fraction) and TiO_2 specimens, namely bare TiO_2 and anion-doped TiO_2 (C-doped TiO_2, N-doped TiO_2, S-doped TiO_2, and N–S co-doped TiO_2) were investigated. Besides DOC, adsorption properties of HA and its molecular size fractions onto bare TiO_2 and anion-doped TiO_2 specimens were also evaluated and compared in terms of the specified and specific UV–vis spectroscopic parameters.

3.1. UV–vis spectral features

Following adsorption, UV–vis spectral features of all of the HA samples displayed a declining trend resembling untreated HA. Therefore, specified UV–vis parameters could be successfully employed in the evaluation of the adsorption properties of HA and its molecular size fractions onto all of the TiO_2 specimens. For comparative reasons, 0.5 mg mL^{-1} adsorbent dose was selected and respective UV–vis spectra were displayed in Fig. 1(A)–(C).

Concurrently, specific UV–vis parameters displayed dopant-type dependent variations in relation to the decreasing DOC contents of the HA molecular size fractions. For simplicity purposes, a fixed adsorbent dose of 0.5 mg mL^{-1} was chosen for the schematic presentation of the variations attained in specific UV–vis parameters (Fig. 2).

From a general perspective, all specific UV–vis parameters displayed similar trends for 0.45 μm filtered and 30 kDa molecular size fractions of HA following adsorption onto N-doped TiO_2 irrespective of the adsorbent dose of TiO_2. All specific parameters displayed similar decreasing trends following adsorption onto C-doped, S-doped TiO_2, and N–S co-doped TiO_2. Moreover, all specific UV–vis parameters exhibited increasing trends for 30 kDa molecular size fractions of HA following adsorption after 0.6 mg mL^{-1} dose of S-doped TiO_2.

SCoA displayed significantly decreasing trend for all of the molecular size fractions of HA following adsorption onto bare TiO_2, the reason of which could be attributed to the effect of color-forming moieties on sorption capacity. On the other hand, SCoA exhibited relatively consistent trend for all of the molecular size fractions of HA following adsorption onto doped TiO_2 (C-doped TiO_2, N-doped TiO_2, S-doped TiO_2, and N–S co-doped TiO_2). Hence, SCoA could not be regarded as discriminative on the evaluation of surface interactions between molecular size fractions of HA and anion-doped TiO_2 specimens. $SUVA_{254}$ displayed slightly decreasing trend in all of molecular size fractions of HA following adsorption onto bare TiO_2. All specific parameters displayed similar trends each other for 100 and 30 kDa molecular size fractions of HA following adsorption onto C-doped TiO_2, while there is a different trend depending on dosage of TiO_2 for 0.45 μm filtered fraction of HA. $SUVA_{254}$ values of greater than 4.0 indicate the presence of a more dense aromatic character of HA [15]. Although variations in $SUVA_{254}$ were obtained with respect to the type of the dopant, it could be visualized that following adsorption could still retain its aromatic character. Moreover, $SUVA_{365}$ and $SUVA_{280}$ followed similar trends to $SUVA_{254}$ expressing the role of the UV absorbing centers on the adsorptive interactions irrespective of the dopant type and adsorbent dose.

3.2. Adsorption isotherm modeling

Adsorption isotherms of HA molecular size fractions in the form of q_A (DOC_{HA}/mass of TiO_2) vs. C_e (equilibrium DOC_{HA}) displayed C-type isotherm with the exception of N–S co-doped TiO_2 [16]. Selected adsorption isotherms of HA molecular size fractions onto bare and C-, N-, and S-doped TiO_2 specimens were given in Fig. 3.

The adsorption isotherms of HA molecular size fraction onto N–S co-doped TiO_2 specimens could be visualized as composed of two regions (Fig. 4).

Region I could be ascribed to the steep region where low doses of TiO_2 (0.1–0.5 mg mL^{-1}) were present for the successive adsorption of humic fractions. Region II could be described as the linear part at which TiO_2 doses were in the range of 0.5–1.0 mg mL^{-1} displaying the presence of excess surface area for HA subfractions. The diverse nature of the N–S co-doped TiO_2 with respect to the mono-doped counterparts could possibly be attributed as the reason for two regional adsorption behaviors. Since N and S atoms are replaced by the surface oxygen atoms of TiO_2, pH-dependent different surface acidic properties could be expected [17].

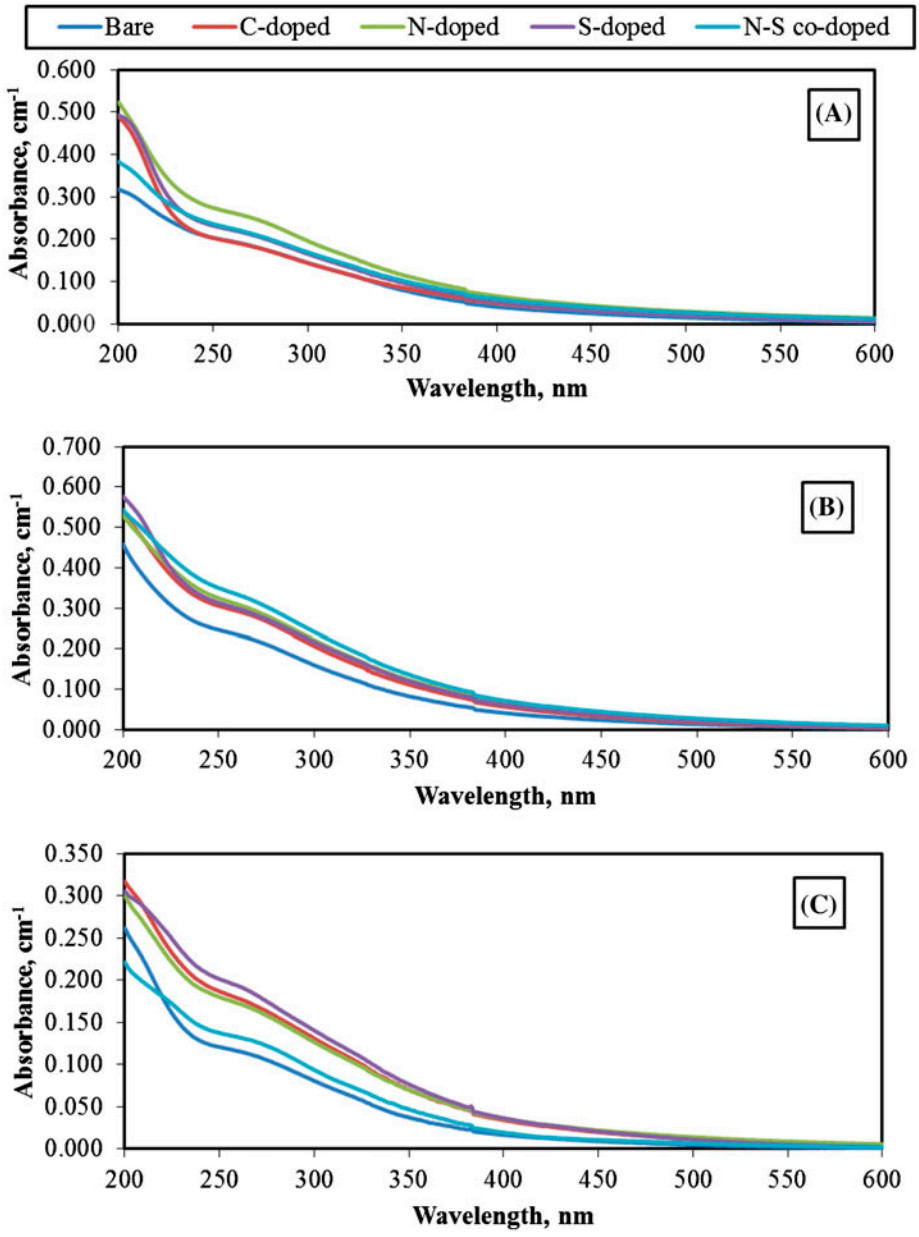

Fig. 1. UV–vis spectra of HA molecular size fractions upon adsorption onto 0.5 mg mL^{-1} bare and doped TiO_2 specimens. (A) 0.45-μm filtered fraction, (B) 100-kDa fraction, and (C) 30-kDa fraction of HA.

Equations preferred to explain the experimental isotherm data were described by Freundlich, Langmuir, and Dubinin–Radushkevich. Freundlich isotherm is a non-linear adsorption equilibrium model expressing the adsorption occurrences on heterogeneous surfaces including diverse adsorption sites with adsorption on each site following Langmuir isotherm [18]. The Freundlich adsorption model can be expressed by the following equation (Eq. (1)):

$$q_A = K_F C_e^{1/n} \quad (1)$$

where C_e (with units of mass/volume, or moles/volume) is the concentration of adsorbate remaining in solution at equilibrium, q_A (with units of mass adsorbate/mass adsorbent, or mole adsorbate/mole adsorbent) expresses the mass of contaminant adsorbed per unit weight of the adsorbent. K_F and $1/n$ are empirical constants deduced from the experimental equilibrium

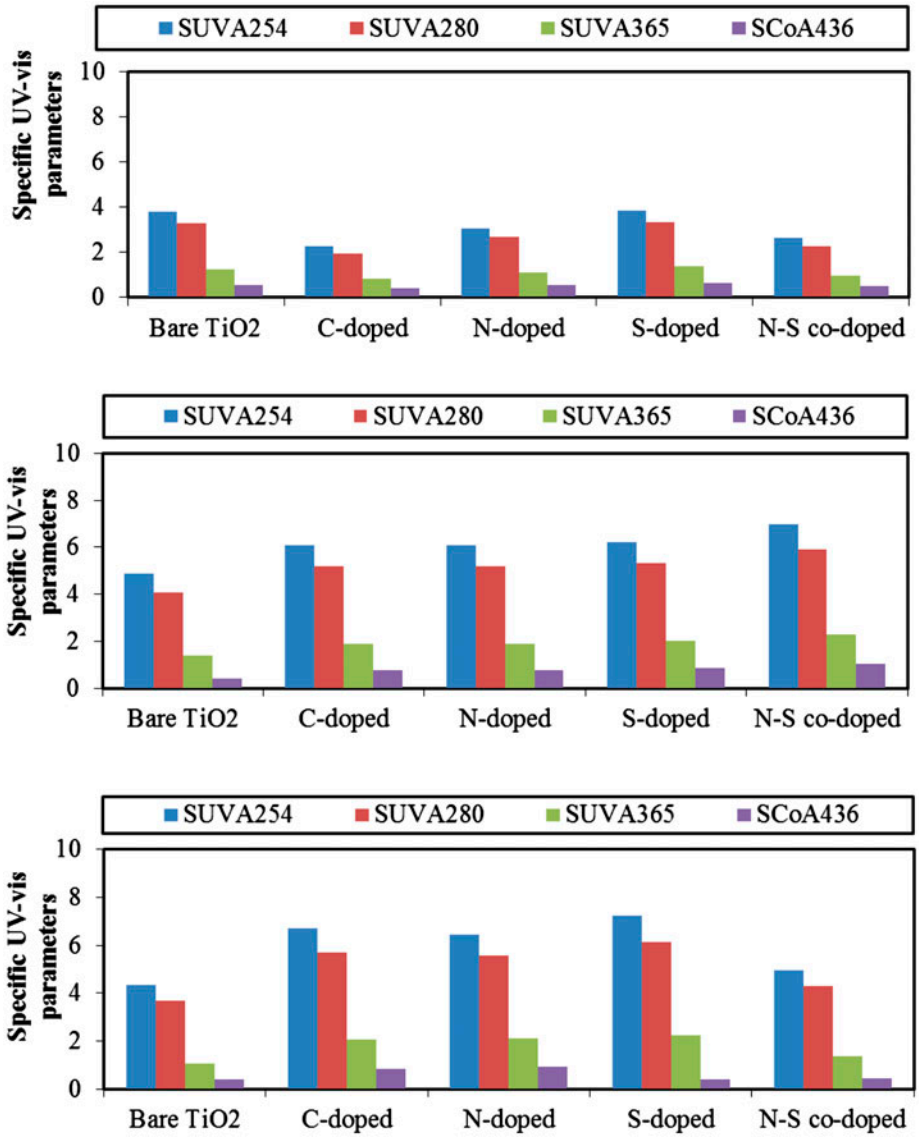

Fig. 2. Specific UV–vis parameters of HA molecular size fractions upon adsorption onto 0.5-mg mL^{-1} bare and doped TiO_2 specimens. (A) 0.45-μm filtered fraction, (B) 100-kDa fraction, and (C) 30-kDA fraction of HA.

adsorption data. The term $1/n$ is function of the strength of adsorption that the rate of the adsorption increases with solute concentration. K_F is related fundamentally to the capacity of the adsorbent for the adsorbate [19].

The Langmuir isotherm model assumes that maximum adsorption corresponds to a saturated monolayer of solute molecules on the adsorbent surface, that the energy of adsorption is constant, and that there is no transmigration of adsorbate in the plane of the surface. In other words, adsorption is limited to monolayer coverage. The Langmuir adsorption model can be expressed by the following equation (Eq. (2)):

$$q_A = \frac{q_{max} K_L C_e}{1 + K_L C_e} \quad (2)$$

where q_A and C_e express the before given meanings, K_L represents an empirical constant, which is called the binding constant, and q_{max} is the maximum quantity adsorbable when all the adsorption sites are occupied [20].

Dubinin–Radushkevic (D–R) isotherm is generally applied at low concentration and can be utilized to describe the adsorption on both heterogeneous and homogeneous surfaces [21,22]. The Dubinin–

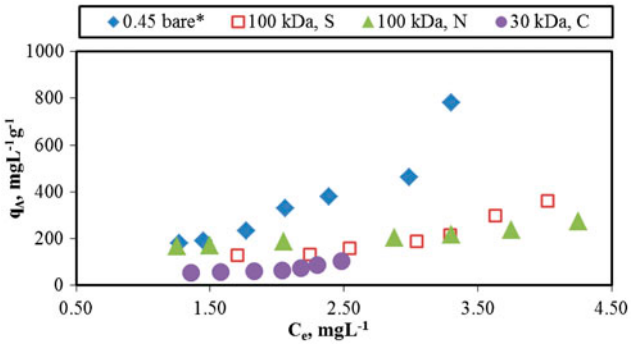

Fig. 3. Adsorption isotherms of 0.45-μm filtered fraction of HA onto bare TiO_2, 100-kDa fraction of HA onto S-doped TiO_2, 100-kDa fraction of HA onto N-doped TiO_2, and 30-kDa fraction of HA onto C-doped TiO_2 (*0.45 bare: 0.45-μm filtered fraction bare).

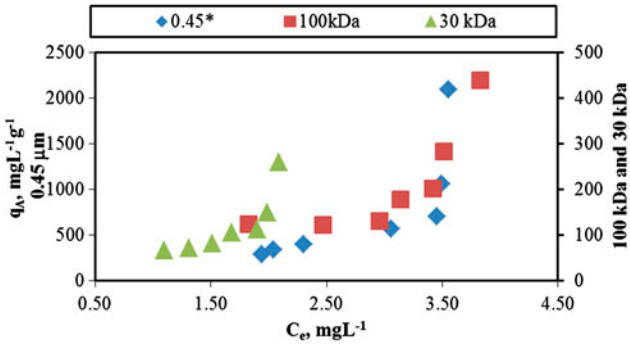

Fig. 4. Adsorption isotherms of molecular size fractions of HA onto N–S co-doped TiO_2 (*0.45: 0.45-μm filtered fraction).

Radushkevic adsorption model can be expressed by the following equation (Eq. (3)):

$$q_A = q_{\max} e^{-\beta\varepsilon^2} \tag{3}$$

where β is the activity coefficient related to mean adsorption energy (mol^2 kJ^{-2}) and ε is the Polanyi potential which equals to;

$$\varepsilon = RT \ln\left(1 + \frac{1}{C_e}\right) \tag{4}$$

where R is the ideal gas constant (8.3145 J mol^{-1} K^{-1}) and T is the absolute temperature in Kelvin (K). q_A and C_e have the same meanings as previously described, but $q_{\max}$ differs from that in the Langmuir model because it represents the total specific micropore volume of the adsorbent. The value of β is related to the adsorption free energy, E (kJ mol^{-1}), which is defined as the free energy change required to transfer 1 mol of ions from solution to the solid surfaces [23]. The relation is as the following:

$$E = \frac{1}{\sqrt{2\beta}} \tag{5}$$

The magnitude of E is useful for estimating the mechanism of the adsorption reaction. If E is in the range of 8–16 kJ mol^{-1}, adsorption is governed by chemical ion exchange. In the case of E is below 8 kJ mol^{-1}, physical forces may affect the adsorption. On the other hand, adsorption may be dominated by particle diffusion if E is higher than 16 kJ mol^{-1} [24,25].

Based on the above given models, all of the adsorption isotherms were modeled to Freundlich (K_F and $1/n$), Langmuir (K_L and $q_{\max}$) as well as Dubinin–Radushkevich ($q_{\max}$, β and E) adsorption isotherm models ($R^2 > 0.70$). Adsorption isotherm model parameters in terms of DOC are displayed in Table 3.

Comparative presentation of the attained results using Freundlich adsorption isotherm model (Eq. (1)) in terms of DOC is displayed in Table 4.

Comparative presentation of the attained results using Langmuir adsorption isotherm model (Eq. (2)) in terms of DOC is displayed in Table 5.

Comparison of the results with respect to the results attained for bare TiO_2 indicated diverse adsorption intensity factors ($1/n$) representing strong concentration dependency of the molecular size fractions of HA. The highest K_F (3.53) and the lowest intensity factor ($1/n = 0.406$) was attained for 100-kDa molecular size fraction of HA adsorption onto N-doped TiO_2. In a similar trend, the highest K_L (1.37) was also attained for adsorption of 30-kDa molecular size fraction of HA onto S-doped TiO_2. The lowest K_L was determined for 30-kDa fraction of HA adsorption onto bare TiO_2. These results emphasized the role of anion doping onto surface properties of TiO_2 acquiring diverse charged species for possible electrostatic attractions.

Furthermore, for a specific dose of TiO_2 (0.5 mg mL^{-1}), BET SA normalized q_A values expressed as DOC_{ads}/SA displayed variations with respect to the molecular size fractions of HA. The following trend could possibly describe the observed differences in a decreasing order; (i) 0.45-μm filtered fraction of HA as N–S co-doped TiO_2 > C-doped TiO_2 > S-doped

Table 3
Adsorption isotherm model parameters expressed in terms of DOC

	Adsorption isotherm model parameters									
	Freundlich model			Langmuir model			Dubinin–Radushkevich			
System	K_F	$1/n$	R^2	K_L	q_{max}	R^2	q_{max}	β	E	R^2
0.45-μm filtered fraction										
Bare TiO_2	2.71	1.49	0.93	0.150	17.1	0.96	5,154	1.40×10^{-8}	5.98	0.93
C-doped TiO_2	1.40	2.37	0.92	0.208	10.4	0.82	369,165	2.34×10^{-8}	4.62	0.92
N-doped TiO_2	1.22	0.797	0.72	0.0469	22.5	0.86	109	8.65×10^{-9}	7.60	0.72
S-doped TiO_2	1.15	1.78	0.82	0.122	13.1	0.74	11,992	1.73×10^{-8}	5.38	0.82
N–S co-doped TiO_2	1.50	2.31	0.76	0.191	12.5	0.91	232,815	2.23×10^{-8}	4.74	0.77
100 kDa fraction										
Bare TiO_2	1.70	1.70	0.94	0.172	10.2	0.94	10,027	1.61×10^{-8}	5.57	0.94
C-doped TiO_2	0.531	1.67	0.72	0.146	3.47	0.72	186	9.70×10^{-8}	7.18	0.72
N-doped TiO_2	3.53	0.406	0.90	0.651	8.45	0.92	28	3.90×10^{-8}	11.3	0.90
S-doped TiO_2	1.39	1.24	0.84	0.128	8.17	0.83	6,438	1.68×10^{-8}	5.46	0.92
N–S co-doped TiO_2	0.873	1.63	0.71	0.187	3.25	0.84	527,023	2.77×10^{-8}	4.25	0.80
30 kDa fraction										
Bare TiO_2	0.894	0.962	0.98	0.0269	34.1	0.98	112	0.90×10^{-8}	7.45	0.98
C-doped TiO_2	0.926	1.01	0.86	0.0447	22.6	0.85	145	9.40×10^{-8}	7.29	0.86
N-doped TiO_2	1.20	1.90	0.93	0.284	3.35	0.96	13,561	1.73×10^{-8}	5.38	0.93
S-doped TiO_2	2.09	0.611	0.70	1.37	3.67	0.91	13	3.30×10^{-8}	12.3	0.92
N–S co-doped TiO_2	1.15	1.79	0.77	0.216	4.81	0.85	777	1.18×10^{-8}	6.51	0.76

Table 4
Freundlich isotherm model parameters expressed in terms of DOC

Model parameters	Comparative presentation of Freundlich isotherm model parameters
0.45 μm filtered fraction	
K_F	Bare TiO_2 > N–S co-doped TiO_2 > C-doped TiO_2 > N-doped TiO_2 > S-doped TiO_2
$1/n$	C-doped TiO_2 > N–S co-doped TiO_2 > S-doped TiO_2 > bare TiO_2 > N-doped TiO_2
100 kDa fraction	
K_F	N-doped TiO_2 > bare TiO_2 > S-doped TiO_2 > N–S co-doped TiO_2 > C-doped TiO_2
$1/n$	Bare TiO_2 > C-doped TiO_2 > N–S co-doped TiO_2 > S-doped TiO_2 > N-doped TiO_2
30 kDa fraction	
K_F	S-doped TiO_2 > N-doped TiO_2 > N–S co-doped TiO_2 > C-doped TiO_2 > bare TiO_2
$1/n$	N-doped TiO_2 > N–S co-doped TiO_2 > C-doped TiO_2 > bare TiO_2 > S-doped TiO_2

TiO_2 > bare TiO_2 > N-doped TiO_2; (ii) 100 kDa fraction of HA as bare TiO_2 > N-doped TiO_2 > S-doped TiO_2 > N–S co-doped TiO_2 > C-doped TiO_2; (iii) 30 kDa fraction of HA as N–S co-doped TiO_2 > S-doped TiO_2 > N-doped TiO_2 > bare TiO_2 > C-doped TiO_2.

The possibility of correlation was explored in between DOC_{ads}/SA and either K_F or K_L in the presence of bare TiO_2 and anion-doped TiO_2 specimens (Fig. 5). Consequently, it could be visualized that DOC_{ads}/SA could not be correlated with either K_F or K_L both with respect to molecular size fraction as well as dopant type.

From TiO_2 specimen type of view, DOC_{ads}/SA correlation to either K_F or K_L could be presented as follows;

Bare TiO_2: decreasing molecular size could be successfully related to both K_F and K_L in a linearly decreasing order.

C-doped TiO_2: decreasing molecular size could be related to K_L in a decreasing trend.

N-doped TiO_2: decreasing molecular size could not be correlated to both K_F and K_L.

S-doped TiO_2: decreasing molecular size could be inversely correlated to both K_F and K_L.

Table 5
Langmuir isotherm model parameters expressed in terms of DOC

Model parameters	Comparative presentation of Langmuir isotherm model parameters
0.45 μm filtered fraction	
K_L	C-doped TiO_2 > N–S co-doped TiO_2 > bare TiO_2 > S-doped TiO_2 > N-doped TiO_2
q_{max}	N-doped TiO_2 > bare TiO_2 > S-doped TiO_2 > N–S co-doped TiO_2 > C-doped TiO_2
100 kDa fraction	
K_L	N-doped TiO_2 > N–S co-doped TiO_2 > bare TiO_2 > C-doped TiO_2 > S-doped TiO_2
q_{max}	Bare TiO_2 > N-doped TiO_2 > S-doped TiO_2 > C-doped TiO_2 > N–S co-doped TiO_2
30 kDa fraction	
K_L	S-doped TiO_2 > N-doped TiO_2 > N–S co-doped TiO_2 > C-doped TiO_2 > bare TiO_2
q_{max}	Bare TiO_2 > C-doped TiO_2 > N–S co-doped TiO_2 > S-doped TiO_2 > N-doped TiO_2

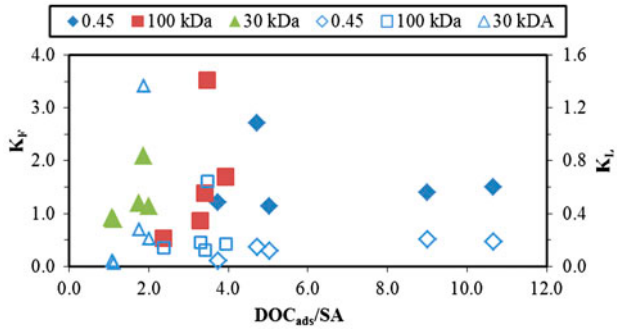

Fig. 5. Correlation between DOC_{ads}/SA with either K_F or K_L in the presence of bare and anion-doped TiO_2 specimens (K_F bold markers and K_L empty markers).

N–S co-doped TiO_2: decreasing molecular size could not be successfully correlated to either K_F or K_L.

It could be deduced that, alterations on the surface properties of the doped TiO_2 specimens displayed diverse adsorptive interactions with humic molecular size fractions.

When the equilibrium data obtained from batch adsorption studies performed at 298 K were fitted to Dubinin–Radushkevich adsorption isotherm model (Eqs. (3)–(5)), the attained model parameters were also displayed in Table 3. From a general perspective with two exceptions, the value of E (E = 4.25−7.60 kJ mol^{-1}) indicated that the main mechanism for the adsorption of diverse molecular size of HA onto bare and anion-doped TiO_2 specimens could be mainly attributed to physical forces. The exceptions were adsorption of 30-kDa fraction of HA onto S-doped TiO_2 (E = 12.3 kJ mol^{-1}) and adsorption of 100-kDa fraction of HA onto N-doped TiO_2 displaying that chemical forces could also be accounted for the surface interactions. All E values being less than 8 kJ mol^{-1} expressing the role of physical forces could be related to the pH_{zpc} condition of the bare as well as doped TiO_2 specimens (Table 2). Since the working pH of the solutions was pH 6.7 ± 0.2 being greater than pH_{zpc} of all TiO_2 specimens, the surface of all of the TiO_2 specimens would attain more positively charged centers. Moreover, under these conditions carboxylic groups present on humic subfractions would be deprotonated acquiring negative charge leading to electrostatic interactions.

The remarkable differences between the values of q_{max} obtained from Langmuir and Dubinin–Radushkevich adsorption isotherm models could be attributed to different definitions of q_{max} in two models. In Langmuir model, q_{max} represents the monolayer coverage, while in Dubinin–Radushkevich model, it represents the total specific micropore volume of the adsorbent. Moreover, the non-presence of a true Langmuirian trend of the adsorption isotherms should also be indicated. It should also be emphasized that all of the adsorbent doses were selected with respect to the photocatalytically active.

As summarized above, Freundlich and Langmuir as well as Dubinin–Radushkevich isotherm model parameters of DOC for 0.45-μm filtration fraction of HA, 100 kDa fraction of HA, and 30 kDa fraction of HA following adsorption onto bare TiO_2 and anion-doped TiO_2 displayed significant differences. The reason could be attributed to the role of the functional groups mainly chromophoric groups present on the different molecular size fractions of HA. Evaluation of the results based on varying molecular size fractions of HA indicated remarkable differences both with respect to the type of the dopant as well as to the morphological character of TiO_2 specimens. In the presence of lower molecular size fraction, Freundlich model displayed that S-doped TiO_2 was more superior to the mono-phase counterpart. The reason could be attributed to the compositional properties of HA subfractions, rather than the alterations in the TiO_2 specimens due to doping.

Referring to the main purpose of the study indicated that the studied loading range of TiO_2 was selected with respect to the photocatalytically active concentration range, the attained results should be carefully interpreted. In this context, the adsorption properties of N-doped TiO_2 specimens should be examined prior to the application of any photocatalytic treatment of strongly adsorbing high molecular weight organic matrix. It should be kept in mind that 0.45-μm filtered fraction of HA was comprised of all humic subfractions. Even the lower molecular size fractions displayed diverse adsorptive properties onto various doped TiO_2 surfaces; the overall effect could be visualized by the data attained for 0.45-μm filtered fraction. The significance of the results attained for 100- and 30-kDa fractions of HA could be related to the diversity of the humic matter as components of NOM present in natural waters.

4. Conclusion

In this study, surface interactions between different molecular size fractions of HA (0.45 μm filtered fraction, 100 kDa fraction, and 30 kDa fraction) and TiO_2 specimens, namely bare TiO_2 and anion-doped TiO_2 (C-doped TiO_2, N-doped TiO_2, S-doped TiO_2, and N–S co-doped TiO_2) were investigated. UV–vis spectral features, specified and specific UV–vis parameters of different molecular size fractions of HA following adsorption were elucidated. Assessment of the results based on varying molecular size fractions of HA pointed out remarkable differences with respect to the type of the dopant. Freundlich, Langmuir, and Dubinin–Radishkovich adsorption isotherm models were successfully employed. Referring to the fundamental aim of the study indicating that the studied dose range of TiO_2 (0.1–1.0 mg mL^{-1}) was selected with respect to the photocatalytically active concentration range, the attained results should be carefully interpreted.

Acknowledgments

Financial support provided by Research Fund of Bogazici University Project No: 6750 is gratefully acknowledged. Moreover, authors would like to thank Professor Zekiye Cinar (Department of Chemistry, Yildiz Technical University) for the preparation of the anion-doped TiO_2 specimens. In addition, authors are grateful to Associate Professor Neren Okte (Department of Chemistry, Bogazici University) for BET analysis of anion doped TiO_2 specimens.

References

[1] G. Davies, E.A. Ghabbour (Eds.), Humic Substances: Structures, Properties and Uses, Royal Society of Chemistry, Cambridge, 1998.
[2] J.P. Croué, J.F. Debroux, G.L. Amy, G.R. Aiken, J.A. Leenheer, Natural organic matter: Structural characteristics and reactive properties, in: P.C. Singer (Ed.), Formation and Control of Disinfection By-products in Drinking Water, AWWA, Denver, CO, 1999, pp. 65–93.
[3] E.T. Gjessing, Physical and Chemical Characteristics of Aquatic Humus, Ann Arbor Science Publishers Inc., Ann Harbor, MI, 1976.
[4] I.H. Suffet, P. MacCarthy, Aquatic Humic Substances: Influence on Fate and Treatment of Pollutants, American Chemical Society, Washington, DC, 1989.
[5] S. Bangkedphol, H.E. Keenan, C.M. Davidson, A. Sakultantimetha, W. Sirisaksoontorn, A. Songsasen, Enhancement of tributyltin degradation under natural light by N-doped TiO_2 photocatalyst, J. Hazard. Mater. 184 (2010) 533–537.
[6] N. Shaham-Waldman, Y. Paz, Modified photocatalysts, in: P. Pichat (Ed.), Photocatalysis and Water Purification: From Fundamentals to Recent Applications, first ed., Wiley-vott Verlang Gmbt & Co KgoA, Weinheim, 2013, pp. 130–143.
[7] Y. Yalcin, M. Kılıç, Z. Cinar, The role of non-metal doping in TiO_2 photocatalysis, J. Adv. Oxid. Technol. 113 (2010) 281–296.
[8] O. Carp, C.L. Huisman, A. Reller, Photoinduced reactivity of titanium dioxide, Prog. Solid State Chem. 32 (2004) 33–177.
[9] C.S. Uyguner, M. Bekbolet, A review on the photocatalytic degradation of humic substances, in: A. Nikolau, H. Selcuk, L. Rizzo (Eds.), Control of Disinfection By-Products in Drinking Water Systems, NOVA Science Publishers Inc., New York, NY, 2007 (Chapter 7.4), pp. 419–446.
[10] N.C. Birben, C.S. Uyguner-Demirel, S. Sen-Kavurmaci, Y.Y. Gurkan, N. Turkten, Z. Cinar, M. Bekbolet, Comparative evaluation of anion doped photocatalysts on the mineralization and decolorization of natural organic matter, Catal. Today 240 (2015) 125–131.
[11] A. Kerc, M. Bekbolet, A.M. Saatci, Effects of oxidative treatment techniques on molecular size distribution of humic acids, Water Sci. Technol. 49 (2004) 7–12.
[12] Y.Y. Gurkan, N. Turkten, A. Hatipoglu, Z. Cinar, Photocatalytic degradation of cefazolin over N-doped TiO_2 under UV and sunlight irradiation: Prediction of the reaction paths via conceptual DFT, Chem. Eng. J. 184 (2012) 113–124.
[13] C.S. Uyguner, M. Bekbolet, Implementation of spectroscopic parameters for practical monitoring of natural organic matter, Desalination 176 (2005) 47–55.
[14] C.S. Uyguner-Demirel, M. Bekbolet, Significance of analytical parameters for the understanding of natural organic matter in relation to photocatalytic oxidation, Chemosphere 84 (2011) 1009–1031.
[15] J.K. Edzwald, W.C. Becker, K.L. Wattier, Surrogate parameters for monitoring organic matter and THM precursors, J. AWWA 77 (1985) 122–132.
[16] C.H. Giles, T.H. MacEwan, S.N. Nakhwa, D. Smith, Studies in adsorption. Part XI. A system of classification of solution adsorption isotherms, and its use in

diagnosis of adsorption mechanisms and in measurement of specific surface areas of solids, J. Chem. Soc. 33(1960) (1960) 3973–3993.
[17] J.A. Rengifo-Herrera, E. Mielczarski, J. Mielczarski, N.C. Castillo, J. Kiwi, C. Pulgarin, *Escherichia coli* inactivation by N, S co-doped commercial TiO_2 powders under UV and visible light, Appl. Catal. B: Environ. 84(3–4) (2008) 448–456.
[18] G.W. vanLoon, S.J. Duffy, Environmental Chemistry: A Global Perspective, third ed., Oxford University Press, New York, NY, 2010, pp. 254–272.
[19] V.L. Snoeyink, R.S. Summers, Adsorption of organic compounds, in: R.D. Letterman (Ed.), Water Quality and Treatment, A Handbook of Community Water Supplies, fifth ed., McGraw-Hill Inc., New York, NY, 1999, pp. 11–83 (Chapter 13).
[20] W.J. Weber, Physicochemical Processes: For Water Quality Control, first ed., Wiley-Interscience, New York, NY, 1972.
[21] T. Shahwan, H.N. Erten, Thermodynamic parameters of Cs^+ sorption on natural clays, J. Radioanal. Nucl. Chem. 253 (2002) 115–120.
[22] T. Shahwan, H.N. Erten, Temperature effects in barium sorption on natural kaolinite and chlorite–illite clays, J. Radioanal. Nucl. Chem. 260 (2004) 43–48.
[23] S. Aksoyoglu, Sorption of U(VI) on granite, J. Radioanal. Nucl. Chem. Art. 134 (1989) 393–403.
[24] R. Donat, A. Akdogan, E. Erdem, H. Cetisli, Thermodynamics of $Pb^{2+}$and Ni^{2+} adsorption onto natural bentonite from aqueous solutions, J. Colloid Interface Sci. 286 (2005) 43–52.
[25] A. Özcan, E.M. Öncü, A.S. Özcan, Kinetics, isotherm and thermodynamic studies of adsorption of Acid Blue 193 from aqueous solutions onto natural sepiolite, Colloids Surf. A 277 (2006) 90–97.